

On optical field driven quantum spin Hall phase in Bi₂Se₃ thin film with magnetic impurities

Udai Prakash Tyagi , Partha Goswami

D. B. College, University of Delhi, Kalkaji, New Delhi, India

uptyagi@yahoo.co.in
physicsgoswami@gmail.com

Received: 3 January 2023;

Accepted: 4 April 2023;

<http://dx.doi.org/10.57647/J.JTAP.2023.1702.31>

Oxford OX29 4DA; GB; <https://oiccpres.com>;

On optical field driven quantum spin Hall phase in Bi₂Se₃ thin film with magnetic impurities

Udai Prakash Tyagi^{1,a*} and Partha Goswami^{2,b}

¹ D.B.College, University of Delhi, Kalkaji, New Delhi-110019, India

² D.B.College, University of Delhi, Kalkaji, New Delhi-110019, India

^auptyagi@yahoo.co.in, ^bphysicsgoswami@gmail.com

Abstract. The normal incidence of circularly polarized optical field (POF) of tunable intensity on the topological insulator Bi₂Se₃ film is shown to give rise to the quantum spin Hall (QSH) effect, in the presence of the magnetic impurities (MI), starting with a low-energy two-dimensional, time-dependent Hamiltonian in the framework of the Floquet theory. The quantized topological number- the Kane–Mele index Z_2 for QSH phase- strongly support this topological state.

Keywords:: Circularly polarized optical field; Floquet theory; Magnetic impurities, Kane–Mele index Z_2 , Quantum spin Hall phase .

Introduction

The strong spin orbit coupling (SOC) is responsible for many of the distinctive properties of topological insulators, such as the compound Bi₂Se₃. For example, the direct backscattering immunity of the surface spin-momentum locked (SML) electrons when coming up against edge or surface defects. The electron energy quantization in these materials is more Dirac-like than bulk-electron-like. In this paper we consider a thin film of Bi₂Se₃ together with magnetic impurities (MI) with normal parallel to the z crystal growth direction. The compound Bi₂Se₃ is generally n-type due to Se vacancies, though it can be transformed to a p-type material by small amounts of alkaline earth metal doping. The compound is based on the stacking of “quintuple layer” building blocks to yield a crystallographic cell with rhombohedral symmetry. The structure parameters are $a = b = 0.41$ nm, $c = 2.853$ nm, $a = b = 90^\circ$, and $\gamma = 120^\circ$. Along the z-direction, Se and Bi hexagonal planes stacked on top of each other in the bulk. The (Se-Bi-Se-Bi-Se) pentagonal layer is the basic building block of thin film structures. The layers interact weakly through van der Waals force.

The model Hamiltonian [1-10] of the system in momentum space could be written down in the basis comprising of the hybridized states of p_z Bi orbital (of odd parity) and p_z Se orbital (of even parity). The hybridization between the orbitals is assumed to be strong. The presence of magnetic impurities (MI) together with strong SOC in Bi₂Se₃ system leads to a QAH state. A common trait of all the QAH system band structure is that those bands, which are close to the Fermi level, correspond to chiral/helical fermions (Dirac-like). The quantum spin Hall (QSH) effect, on the other hand, is a spin genre of quantum Hall effect. A twisted Hilbert space is one of the characteristics of a QSH system which leads to a pair of counter-propagating helical edge states with opposite spins under topological protection. This leads to inducement of a transverse spin current near the system boundary due to an electric current. Such abstruse states with SML gives rise to two-dimensional strong topological insulator. *In what follows we show that emergent quantum spin Hall (QSH) phase [11] is possible by the normal incidence of circularly polarized optical field (CPOF) on our system though we have broken time reversal symmetry (TRS) due to the presence of MI.* For this purpose, we impart the time-dependence to our low-energy two-dimensional model Hamiltonian. The time dependence arises due to circularly polarized optical light (POF) describable by the associated electromagnetic gauge field. The coupling between the lattice electrons and the gauge field is established by the Peierls substitution. We make use of the Floquet theory, where a time-dependent problem is mapped into a stationary one [12,13] in terms of quasi-energies. We use this theory in the high-frequency limit. Interestingly, the optical field tuneability leads to the emergence of QSH phase in the presence of MI, when intensity of the incident radiation is high, from the quantum anomalous Hall phase. The

conclusive evidence of this emergence is obtained calculating the topological index Z_2 . It is worth mentioning that periodic POF provides a potent way to carry out theoretical proposition and experimental realization, detection, and manipulation of diverse novel optical and electronic properties and applications of materials, such as the polarization-dependent optoelectronic device applications in 2D materials and their heterostructures [14], the topological phase transitions in semimetals [15,16], the Floquet engineering of magnetism in topological insulator thin films [17,18], and so on. The Floquet theory leads to a highly powerful means to engineer, and detect exotic Floquet topological phases with a high tunability. We model the interaction between the itinerant electrons in the system and impurity moment with the coupling term $(J) \sum_j S_j \cdot s_j$, where S_j is the j th-site impurity spin, $s_j = \left(\frac{1}{2}\right) d_{j\sigma}^\dagger \tau_z d_{j\sigma}$, $d_{j\sigma}^\dagger$ is the fermion creation operator at site- j , spin-state σ ($=\uparrow, \downarrow$), and τ_z is the z-component of the Pauli matrices. For $|\mathbf{S}| > 1$, we can make the approximation of treating the impurity spins as classical vectors. Upon doing so, we write $M = |J| |\mathbf{S}|$ where we absorb the magnitude of the impurity spin into the coupling constant J .

We have organized the paper in the following manner: In section 2, we present a model for a TI in the basis of the hybridized states of p_z Bi orbital (of odd parity) and p_z Se orbital (of even parity). The energy eigenvalues of the insulator surface and the eigenvectors corresponding to these values are calculated. In section 3, we study the interaction of the TI film with normally incident POF in the framework of the Floquet formalism which transforms our time-dependent Hamiltonian into a time-independent Hamiltonian represented by an infinite matrix. The paper ends with a brief concluding remark in section 4.

2. Surface State Hamiltonian

The Bi_2Se_3 thin films have been attracted a lot due to their unique electrical and optical properties. This enables the development of topological insulator-based devices and applications including thermoelectric, and optoelectronics devices. In this section, we consider a thin film of Bi_2Se_3 together with magnetic impurities with normal parallel to the z crystal growth direction. We denote the thickness of the thin film (along z direction) as W . Accordingly, the corresponding Hamiltonian $H(\mathbf{k})$ given below contains constant terms and the z derivatives. In the basis $\left(\left| p_{1z,\uparrow}^{\text{even}} \right\rangle \left| p_{2z,\uparrow}^{\text{odd}} \right\rangle \left| p_{1z,\downarrow}^{\text{even}} \right\rangle \left| p_{2z,\downarrow}^{\text{odd}} \right\rangle \right)$ of the hybridized states of p_z Se orbital (of even parity) and p_z Bi orbital (of odd parity), the momentum space dimensionless model Hamiltonian [1-10] of the system could be written as

$$H(\mathbf{k}) = (\epsilon(\mathbf{k}) \sigma_0 + M \sigma_z) \otimes \tau_0 + \vartheta(\mathbf{k}) \sigma_0 \otimes \tau_z + A_1 \{ (a_x k_x \sigma_x + a_y k_y \sigma_y) + \eta a_z k_z \sigma_z \} \otimes \tau_x, \quad (1)$$

where in the ket $\left| p_{z,\sigma}^{\text{even/odd}} \right\rangle$ the symbol $\sigma = \uparrow \downarrow$ stands for the real spin, $k = (k_x, k_y)$, $\eta < 1$, M is the exchange field from the magnetic dopants, $\sigma_{x,y,z}$, and $\tau_{x,y,z}$, respectively, are the Pauli matrices for the spin and the orbital degrees of freedom. If one wishes to work with a lattice model, the following replacements are necessary: $a_j k_j \rightarrow \sin(a_j k_j)$ and $(a_j^2 k_j^2) \rightarrow 2(1 - \cos(a_j k_j))$ where $j = (x, y, z)$, and a_j is the lattice constant along j direction. It may be mentioned that the lattice constants of bulk Bi_2Se_3 are in the basal plane $a = 4.14 \text{ \AA}$ and along the c -axis $c = 28.64 \text{ \AA}$. Here $a_x = a_y = a$ and $a_z = c$. The energies $\epsilon(k) = \epsilon_0 - D_1 c^2 \partial_z^2 + D_2 a^2 k^2$, and $\vartheta(k) = \vartheta_0 + B_1 c^2 \partial_z^2 - B_2 a^2 k^2$, and $k^2 = (k_x^2 + k_y^2)$. Thus, it is easy to see that the coefficients B_2 and D_2 serve as the first neighbor hopping in a lattice model. Here ϑ_0 denotes the term, whose magnitude corresponds to that of the band gap. D_2 corresponds to conduction and valence band curvatures. A_1 is the strength of hybridization between the orbitals. Furthermore, $\vartheta_0/B_2 > 0$ ($\vartheta_0/B_2 < 0$) corresponds to the topologically nontrivial (trivial) phase. A transition between these topologically distinct sectors occurs at $\vartheta_0 = 0$,

accompanied by a band-gap closing at $k = 0$. We have made the Hamiltonian dimensionless by dividing every term in $H(\mathbf{k})$ by the first neighbor hopping $B_2 = 3.31 \text{ eV}$ [1,2] which is the highest energy value. In this scheme we have $\epsilon_0 = -0.003, A_1 = 0.31, \eta = 0.16, B_1 = 0.18, B_2 = 1, M = 0.08, D_1 = 0.024$, and $D_2 = 0.34$ following the values of these quantities given in ref. [1,2].

In order to obtain surface state Hamiltonian ($H^{surface}(k, \lambda)$) we make the replacement $ck_z \rightarrow -ic \partial_z$ and look for states localized within the surface of the form $exp(-i\lambda z)$. Under the open boundary condition(OBC), we seek such a value of λ for which this exponential will be vanishingly small for $z = \pm \frac{W}{2}$. From above we find $H^{surface}(k, \lambda) = (\epsilon_1(k, \lambda) \sigma_0 + M \sigma_z) \otimes \tau_0 + \vartheta(k, \lambda) \sigma_0 \otimes \tau_z + A_1 \{ (ak_x \sigma_x + ak_y \sigma_y) - \eta c \lambda \sigma_z \} \otimes \tau_x$, where $\epsilon_1(k, \lambda) = \epsilon_0 + D_1 c^2 \lambda^2 + D_2 a^2 k^2$, and $\vartheta(k, \lambda) = \vartheta_0 - B_1 c^2 \lambda^2 - B_2 a^2 k^2$. It is worth mentioning that if one intends to take disorder into consideration, one may replace $\epsilon_1(k, \lambda)$ in the Hamiltonian above by $\epsilon(k, \lambda) = (\epsilon_1(k, \lambda) + \Gamma_0)$ where Γ_0 corresponds to a random disorder potential (RDP) which has continuous uniform distribution in the interval $[-\Gamma/2, \Gamma/2]$ with a positive parameter Γ . If a uniform distribution is continuous (discrete), it has an infinite (finite) number of equally likely measurable values. The eigenvalues (ϵ_j) of this matrix is given by the quartic $\epsilon_j^4 + \gamma_3(k, \lambda) \epsilon_j^3 + \gamma_2(k, \lambda) \epsilon_j^2 + \gamma_1(k, \lambda) \epsilon_j + \gamma_0(k, \lambda) = 0$ where

$$\begin{aligned} \gamma_0(k, \lambda) &= (\eta A_1 c \lambda)^4 + 2(\eta A_1 c \lambda)^2 ((A_1 a k)^2 + \vartheta^2(k) - \epsilon^2(k) - M^2) \\ &\quad + ((A_1 a k)^2 + \vartheta^2(k))^2 - 2(A_1 a k)^2 (\epsilon^2(k) - M^2), \\ \gamma_1(k, \lambda) &= 4((\eta A_1 c)^2 \lambda^2 + (A_1 a k)^2) \epsilon(k) + 4(\vartheta^2(k) \epsilon(k) - \epsilon^3(k) + \epsilon(k) M^2), \\ \gamma_2(k, \lambda) &= -2((\eta A_1 c)^2 \lambda^2 + (A_1 a k)^2) - 2(\vartheta^2(k) - 3\epsilon^2(k) + M^2), \gamma_3(k, \lambda) = -4\epsilon(k). \end{aligned}$$

In view of the Ferrari's solution of a quartic equation, we find the roots as

$$\epsilon_j(s, \sigma, k, \lambda) = \sigma \sqrt{\frac{\eta_0(k, \lambda)}{2} - \frac{\gamma_3(k, \lambda)}{4}} + s \left(b_0(k, \lambda) - \left(\frac{\eta_0(k, \lambda)}{2} \right) + \sigma c_0(k, \lambda) \sqrt{\frac{2}{\eta_0(k, \lambda)}} \right)^{\frac{1}{2}}, \quad (2)$$

where $j = 1, 2, 3, 4$, $\sigma = \pm 1$ is the spin index and $s = \pm 1$ is the band-index. Since, the spin index σ occurs twice in Eq. (3), the term $\sqrt{\frac{\eta_0(k, \lambda)}{2}}$ does not act like magnetic energy. The functions appearing in (3) are given by

$$\eta_0(k, \lambda) = \frac{2b_0(k, \lambda)}{3} + (\Delta(k, \lambda) - \Delta_0(k, \lambda))^{\frac{1}{3}} - (\Delta(k, \lambda) + \Delta_0(k, \lambda))^{\frac{1}{3}},$$

$$\Delta_0(k, \lambda) = \left(\frac{b_0^3(k, \lambda)}{27} - \frac{b_0(k, \lambda)d_0(k, \lambda)}{3} - c_0^2(k, \lambda) \right),$$

$$\Delta(k) = \left(\frac{2}{729} b_0^6 + \frac{4d_0^2 b_0^2}{27} + c_0^4 - \frac{d_0 b_0^4}{81} - \frac{2b_0^3}{27} + \frac{2c_0^2 b_0 d_0}{3} + \frac{d_0^3}{27} \right)^{1/2},$$

$$b_0(k, \lambda) = \left\{ \frac{3\gamma_3^2(k, \lambda) - 8\gamma_2(k, \lambda)}{16} \right\}, c_0(k, \lambda) = \left\{ \frac{-\gamma_3^3(k, \lambda) + 4\gamma_3(k, \lambda)\gamma_2(k, \lambda) - 8\gamma_1(k, \lambda)}{32} \right\}$$

$$d_0(k, \lambda) = \frac{-3\gamma_3^4(k, \lambda) + 256\gamma_0(k, \lambda) - 64\gamma_3(k, \lambda)\gamma_1(k, \lambda) + 16\gamma_3^2(k, \lambda)\gamma_2(k, \lambda)}{256}. \quad (3)$$

The eigenvectors corresponding to the energy eigenvalues $\epsilon_j(s, \sigma, k, \lambda)$ are

$$|u^{(j)}(k, \lambda, z)\rangle = \zeta_j^{-1/2}(k, \lambda) \exp(-i\lambda z) \begin{pmatrix} \psi_1^j(k, \lambda) \\ \psi_2^j(k, \lambda) \\ \psi_3^j(k, \lambda) \\ \psi_4^j(k, \lambda) \end{pmatrix}, \quad j=1, 2, 3, 4, \quad (4)$$

$$\zeta_j(k, \lambda) = |\psi_1^j(k)|^2 + |\psi_2^j(k)|^2 + |\psi_3^j(k)|^2 + |\psi_4^j(k)|^2$$

$$\psi_1^j(k, \lambda) = 1, \quad \psi_v^j(k, \lambda) = \Delta_v^{(j)}(k, \lambda) / \Delta^{(j)}(k, \lambda), \quad v=2, 3, 4$$

$$\Delta_2^{(j)}(k, \lambda) = ((A_1 a k_-))[(A_1 a k)^2 + (\eta A_1 c \lambda)^2] - \left((\epsilon_j(s, \sigma, k, \lambda) - \epsilon(k))^2 - (M + \vartheta(k))^2 \right)$$

$$\Delta_3^{(j)}(k, \lambda) = -(\eta A_1 c \lambda)^2 \{ \epsilon_j(s, \sigma, k, \lambda) - \epsilon(k) + M + \vartheta(k) \}$$

$$- \left((\epsilon_j(s, \sigma, k, \lambda) - \epsilon(k))^2 - (M + \vartheta(k))^2 + (A_1 a k)^2 \right) \{ \epsilon_j(s, \sigma, k, \lambda) - \epsilon(k) - M + \vartheta(k) \}$$

$$\Delta_4^{(j)}(k, \lambda) = -(\eta A_1 c \lambda)(A_1 a k)^2 + ((\eta A_1 c \lambda)^3) -$$

$$- \{ (\epsilon_j(s, \sigma, k, \lambda) - \epsilon(k) - M)^2 - \vartheta^2(k) \} (\eta A_1 c \lambda)$$

$$\Delta^{(j)}(k, \lambda) = (2M(\eta A_1 c \lambda)(A_1 a k_-)). \quad (5)$$

These eigenvectors specify surface states. The wave number λ is an unknown in Eq. (2). As already stated under OBC, we seek solution for this in the form $(\pm ib)$, $b > 0$, for ensuring an exponentially decaying term with plus sign for $z < 0$ (minus sign for $z > 0$) in the surface states. To determine an approximate value of λ graphically we first write the energy eigenvalue equation given by the quartic above as an equation for $x = \lambda^2$, for a given energy eigenvalue E_f , at the Γ point. We obtain a quartic given as $B_1 x^4 + A x^3 + B x^2 + C(M)x + D(M) = 0$. Here

$$A = [2(\eta A_1)^2 B_1^2 + (\eta A_1)^2 D_1^2 + B_1^2 D_1 E_f - 4D_1^3 E_f - 2\vartheta_0 B_1^3],$$

$$B = [(\eta A_1)^4 - 4(\eta A_1)^2 \vartheta_0 B_1 + 2(\eta A_1)^2 \epsilon_0 D_1 + 4(\eta A_1)^2 D_1 E_f + 3(2D_1^2 - B_1^2) E_f^2$$

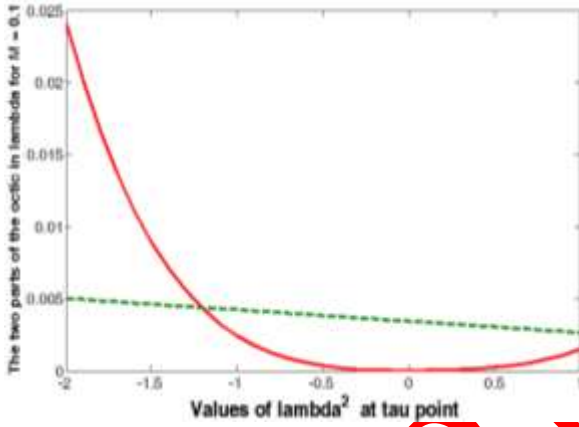
$$- 12\epsilon_0 D_1^2 E_f + 4\epsilon_0 B_1^2 E_f - 8\vartheta_0 B_1 D_1 E_f + 6\vartheta_0^2 B_1^2],$$

$$C(M) = [4(\eta A_1)^2 \epsilon_0 E_f + (\epsilon_0^2 + M^2)(\eta A_1)^2 + 2(\eta A_1)^2 \vartheta_0^2 - 2\vartheta_0 B_1^3 - 2(\eta A_1)^2 E_f^2 + 2\epsilon_0 D_1 E_f^2$$

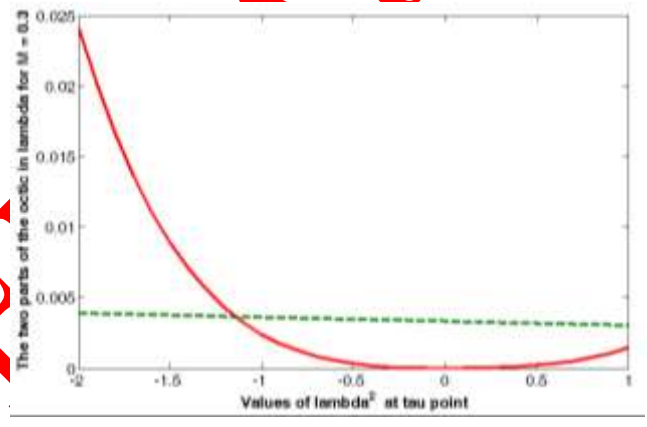
$$- 2\vartheta_0 B_1 E_f^2 - 4D_1 E_f^3 + 4D_1 E_f M^2 - 12\epsilon_0^2 D_1 E_f - 8\vartheta_0 B_1 \epsilon_0 E_f + 4\vartheta_0^2 D_1 E_f],$$

$$D(M) = [E_f^4 + \vartheta_0^4 - 2\vartheta_0^3 B_1 + 4\epsilon_0 E_f M^2 - 4\epsilon_0^3 E_f + 4\epsilon_0 \vartheta_0^2 E_f + 6\epsilon_0^2 E_f^2 - 12M^2 E_f^2 - 12\vartheta_0^2 E_f^2 - 4\epsilon_0 E_f^3]; \quad (6)$$

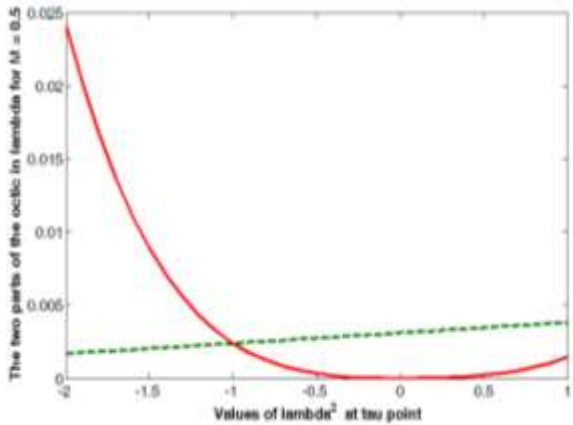
the coefficients C (D) is increasing (decreasing)function of the exchange field M. Next, we plot $f_1=B_1x^4 + Ax^3 + Bx^2$ and $f_2 = C(M)x + D(M)$ as functions of the dimensionless number $x = (c\lambda)^2$ for a given M. In Figure 1 these plots are shown for M = 0.10 , 0.30, 0.50, and 0.80. As the value of M increases, the point of intersection of the two curves (which corresponds a solution sought for of the equation $B_1x^4 + Ax^3 + Bx^2 + C(M)x + D(M) = 0$) shifts to the right. In Figure 1(e) we have shown a plot of $\exp(-b(\frac{z}{c}))$ as a function of (z/c) where $b \approx 1$ for M = 0.5 (see Figure 1(c)). It is clear from the from Figure 1(e) that a thickness of the film (W/c) must be of O(10) to ensure surface state practically equal zero at $z = \pm \frac{W}{2}$. Since $c = 28.64 \text{ \AA}$, the thickness may be taken as $W \approx 30 \text{ nm}$. In the next section we discuss the effect of the normal incidence of circularly polarized optical field (CPOF)on the film. We shall assume the frequency of the incident light as $2.3 \times 10^{14} \text{ Hz}$ and there-



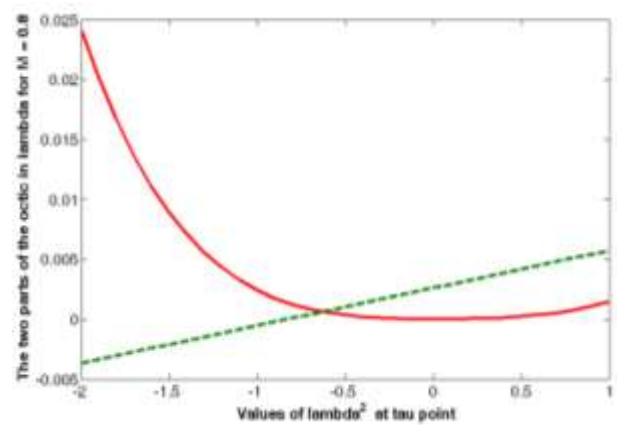
(a)



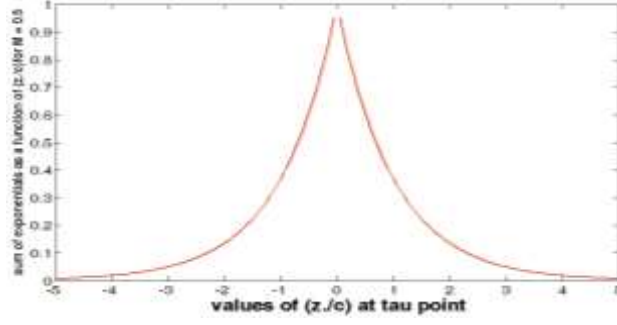
(b)



(c)



(d)



(e)

Figure 1. (a)-(d) The plots of $f_1 = B_1x^4 + Ax^3 + Bx^2$ (in red ink) and $f_2 = C(M)x + D(M)$ (in green ink) as functions of the $(\lambda)^2$ for a given M. (a) $M = 0.10$ (b) $M = 0.30$ (c) $M = 0.50$ and (d) $M = 0.80$. The point of intersection of the two curves corresponds to a solution sought for of the equation $B_1x^4 + Ax^3 + Bx^2 + C(M)x + D(M) = 0$. The numerical values of the parameters are $\epsilon_0 = -0.003$, $A_1 = 0.31$, $\eta = 0.16$, $B_1 = 0.18$, $B_2 = 1$, $E_1 = 0.05$, $D_1 = 0.024$, and $D_2 = 0.34$. (e) A plot of $\exp(-b(\frac{z}{c}))$ as a function of (z/c) where $b \approx 1$ for $M = 0.5$ (see Figure 1(c)).

fore the ratio $W/\lambda_{in} \approx 0.023 \ll 1$, where $\lambda_{in} \approx 1300 \text{ nm}$ is the wavelength of the incident radiation. In the next section we use the Floquet theory in the high-frequency limit of the incident radiation to investigate the system.

3. Floquet Theory

The circularly polarized optical radiation of wavelength λ_{in} incident is supposedly incident on the thin film of Bi_2Se_3 of thickness W where $\lambda_{in}/W \gg 1$. We assume the normal incidence. Suppose the angular frequency of the optical field incident on the film is $\omega = 2\frac{\pi}{T}$ where T is the time period. We also assume that the wavelength λ_{in} of the radiation is much larger than the film thickness W . Upon taking the periodic optical field perturbation into account the hermitian Hamiltonian H^{surface} becomes time periodic too ($H^{\text{surface}}(t) = H^{\text{surface}}(t + T)$). This stipulation is similar to that in the Bloch theory where a spatially periodic potential changes the Bloch function into spatially periodic function with the same periodicity. The Floquet theory is now applied to our time-periodic Hamiltonian operator. As in the Bloch theory (where we replace real momentum by quasi-momentum), the wave function, in terms of the quasi-energies ϵ , has the form $\Psi(t) = \sum_{\nu} \exp\left(-i\left(\frac{\epsilon}{\hbar} + \nu\omega\right)t\right)\psi_{\nu}$ where ν is an integer. The element $H_{\mu,\nu}^{\text{surface}}$ of the Hamiltonian is given by $\sum_{\nu} H_{\mu,\nu}^{\text{surface}}\psi_{\nu} = \epsilon\psi_{\mu}$, where $H_{\mu,\nu}^{\text{surface}} = \mu\hbar\omega\delta_{\mu,\nu} + \frac{1}{T}\int_0^T H^{\text{surface}}(t)e^{i(\mu-\nu)\omega t} dt$, where (μ, ν) are integers. This is the Floquet surface state Hamiltonian of the Bi_2Se_3 thin film. With $\mu \neq \nu$, one can write the matrix as

$$H^{\text{surface}} = \begin{pmatrix} \dots & \dots & \dots & \dots & \dots \\ \dots & H_{-1,-1}^{\text{surface}} & H_{-1,0}^{\text{surface}} & H_{-1,1}^{\text{surface}} & \dots \\ \dots & H_{0,-1}^{\text{surface}} & H_{0,0}^{\text{surface}} & H_{0,1}^{\text{surface}} & \dots \\ \dots & H_{1,-1}^{\text{surface}} & H_{1,0}^{\text{surface}} & H_{1,1}^{\text{surface}} & \dots \\ \dots & \dots & \dots & \dots & \dots \end{pmatrix}. \quad (7)$$

A time-varying gauge field $A(t) = A_0(\sin(\omega t), \sin(\omega t + \varphi))$ represents CPOF. In particular, when the phase $\varphi = \pi$ or 0 , the optical field is linearly polarized. When $\varphi = -\pi/2$ ($\varphi = +\pi/2$), the optical

field is right-handed (left-handed) circularly polarized. Once we have included a gauge field, it is necessary that we make the Peierls substitution $H^{surface}(t) = H^{surface}\left(\mathbf{k} - \frac{e}{\hbar}\mathbf{A}(t)\right)$. In view of the Floquet formalism in ref. [19-24] our system now can be described by a time-independent effective Hamiltonian $H_{eff}^{surface}$ in the high-frequency limit, where

$$H_{eff}^{surface} = (\epsilon(\overline{k}, \lambda)\sigma_0 + M\sigma_z) \otimes \tau_0 + \vartheta(\overline{k}, \lambda) \sigma_0 \otimes \tau_z + \{\widetilde{A}_1(ak_x\sigma_x + ak_y\sigma_y) - \eta\widetilde{A}_1c\lambda\sigma_z\} \otimes \tau_x, \quad (8)$$

Here,

$$\begin{aligned} \epsilon(\overline{k}, \lambda) &= \epsilon(k, \lambda) + \alpha^2 A_0^2 D_2, \quad \vartheta(\overline{k}, \lambda) = \vartheta(k, \lambda) - \alpha^2 A_0^2 B_2 \mp \left(\frac{\alpha^2 A_0^2}{\hbar\omega}\right) A_1^2, \\ \widetilde{A}_1 &= A_1 \left(1 \mp 2B_2 \left(\frac{\alpha^2 A_0^2}{\hbar\omega}\right)\right), \quad \epsilon(k, \lambda) = \epsilon_0 + D_1 c^2 \lambda^2 + D_2 \alpha^2 k^2, \quad \alpha = \frac{e a \omega}{B_2}, \\ \vartheta(k, \lambda) &= \vartheta_0 - B_1 c^2 \lambda^2 - B_2 \alpha^2 k^2. \end{aligned} \quad (9)$$

The value of $\alpha^2 A_0^2$ (this quantity is the intensity of the radiation) is taken to be 0.65 – 0.90 which is good for the radiation field of frequency $\nu \sim 4 \times 10^{14}$ Hz under consideration. Moreover, + sign (– sign) prefixed corresponds to the left handed (right-handed) circularly polarized radiation. The eigenvalues (E_j) of this matrix is given by the quartic

$$E_j^4 + \gamma_{3F}(k, b)E_j^3 + \gamma_{2F}(k, b)E_j^2 + \gamma_{1F}(k, b)E_j + \gamma_{0F}(k, b) = 0 \quad (10)$$

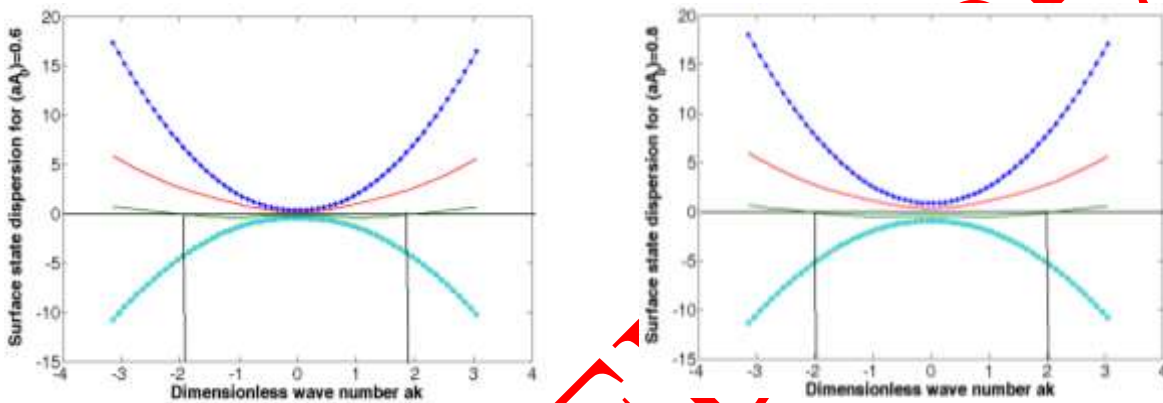
where

$$\begin{aligned} \gamma_{0F}(k, b) &= (\eta A_1 c)^4 b^4 - 2(\eta A_1 c)^2 ((\widetilde{A}_1 a k)^2 + \vartheta(\overline{k}, b)^2 - \epsilon(\overline{k}, b)^2 - M^2) b^2 \\ &\quad + ((\widetilde{A}_1 a k)^2 + \vartheta(\overline{k}, b)^2)^2 - 2(\widetilde{A}_1 a k)^2 (\epsilon(\overline{k}, b)^2 - M^2), \\ \gamma_{1F}(k, b) &= 4(-(\eta A_1 c)^2 b^2 + (\widetilde{A}_1 a k)^2) \epsilon(\overline{k}, b) + 4(\vartheta(\overline{k}, b)^2 \epsilon(\overline{k}, b) - \epsilon(\overline{k}, b)^3 + \epsilon(\overline{k}, b) M^2), \\ \gamma_{2F}(k, b) &= 2((\eta A_1 c)^2 b^2 - (\widetilde{A}_1 a k)^2) - 2(\vartheta(\overline{k}, b)^2 - 3\epsilon(\overline{k}, b)^2 + M^2), \quad \gamma_{3F}(k, b) = -4\epsilon(\overline{k}, b). \end{aligned} \quad (11)$$

We now invoke the Ferrari's solution of a quartic equation(10). We find the roots E_j similar to Eq. (2) albeit with the replacements $\lambda \rightarrow (\pm ib), b > 0, \epsilon_j(s, \sigma, k, \lambda) \epsilon_k - M \rightarrow \epsilon(\overline{k}, b), \vartheta(k) \rightarrow \vartheta(\overline{k}, b)$, and $A_1 \rightarrow \widetilde{A}_1$, as it is evident from Eq. (9). The corresponding eigenvectors are given by Eq.(5) with the same replacements. In Figure 2 (a) we have plotted these energy eigenvalues E_j as a function of (ak) for a given $\alpha A_0 = 0.60$. In Figure 2(b), however, the value of $\alpha A_0 = 0.80$. The value of the other parameters are $\epsilon_0 = -0.003, A_1 = 0.31, \eta = 0.16, B_1 = 0.18, B_2 = 1, M = 0.30, D_1 = 0.024, D_2 = 0.34$, and $\mu = 0$. Here μ is the chemical potential of the fermion number. We find that the band structure does not change much when the exchange energy M is increased from 0.3 upto 0.6. Also, with mild random disorder potential ($W_0 < 1$) we have not noticed any significant change in the band structure. The 3D plots of $E_{31} = \epsilon(s = -1, \sigma = +1, k, \lambda)$, as a function of the

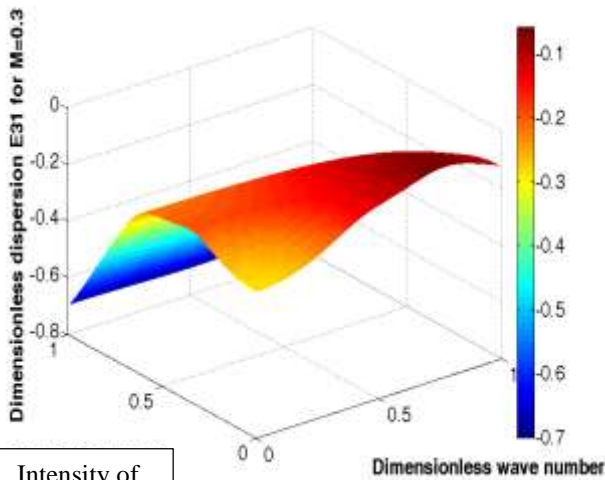
dimensionless wave number (ak) and the intensity of the incident radiation $(\alpha A_0)^2$ (left handed as well as right handed CPOF), are shown in Figures 2(c) and 2(d). As the latter is increased the system makes a crossover to QSH state (blue) starting from quantum anomalous Hall (QAH) state (red). The mild disorder potential ($\Gamma_0 < 1$) is found to have no significant effect on the film band structure.

It must be mentioned that the time reversal symmetry (TRS) identity $H^{surface}(-k_x, -k_y) = \Theta H^{surface}(k_x, k_y) \Theta^{-1}$ is satisfied by the 2D surface state Hamiltonian of TI (or QSH insulator), where the anti-unitary operator $\Theta = \sum_j K$ and $\Sigma_j = \begin{pmatrix} \sigma_j & 0 \\ 0 & \sigma_j \end{pmatrix}$ and σ_j are Pauli matrices. When, for a TRS complaint system, a momentum $+\mathbf{k}$ satisfies the relation $\mathbf{k} + \mathbf{G} = -\mathbf{k}$, where \mathbf{G} is a reciprocal lattice vector, $+\mathbf{k}$ becomes equivalent to $-\mathbf{k}$ due to the periodicity of the BZ. The degeneracy of the momentum pair ($\pm\mathbf{k}$), called Kramer pair, accrues from TRS. These momenta are referred to as the TR-invariant momentum (TRIM). We consider now Figures 2(a) and 2(b). A look-over yields that, in

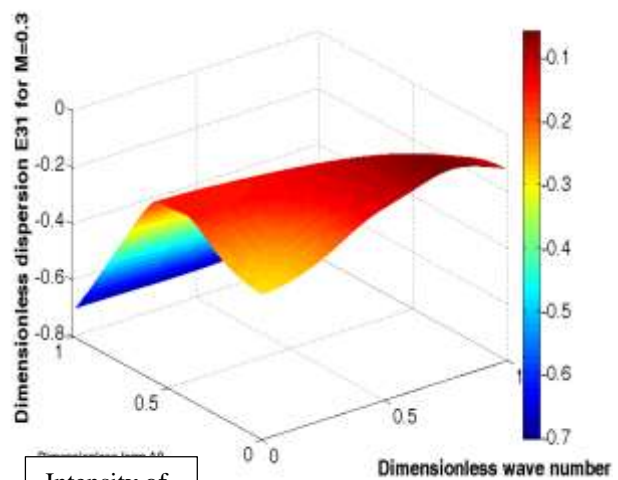


(a)

(b)



Intensity of
CPOF



Intensity of
CPOF

(c) Left handed CPOF

(d) Right handed CPOF

Figure 2. (a),and (b) The plots of E_j as functions of the dimensionless wave number (ak) for a given (αA_0). The numerical values of the other parameters are $\epsilon_0 = -0.003, A_1 = 0.31, \eta = 0.16, B_1 = 0.18, B_2 = 1, E_f = 0.05, D_1 = 0.024, \mu = 0, M = 0.30, \Gamma_0 = 0.3,$ and $D_2 = 0.34$. The Fermi energy $E_F = 0$ is represented by a horizontal line. **(c),and(d)** The 3D plots of $E_{31} = \epsilon(s = -1, \sigma = +1, k, \lambda)$ as a function of the dimensionless wave number (ak) and the intensity of the incident radiation $(\alpha A_0)^2$ (left handed as well as right handed CPOF). As the latter is increased the system makes a crossover to QSH state (blue) starting from quantum anomalous Hall (QAH) state (red).

the band in Figure 2(b), particularly, the band $E_{31} = \epsilon(s = -1, \sigma = +1, k, \lambda)$ possesses the above mentioned momentum $\mathbf{k}_{trim} = (\pm 2, 0), (0, \pm 2)$ (In Figure 2(a), however, this is not true). The reason is that \mathbf{k}_{trim} (referred to as TRIM) satisfies the condition $\mathbf{k}_{trim} + \mathbf{G} = -\mathbf{k}_{trim}$. The vector \mathbf{G} here is equal to $(\mp 4, 0)$ or $(0, \mp 4)$. Let us now note that the Fermi energy $E_F \approx \mu = 0$ inside the gap intersects the surface state band $E_{31} = \epsilon(s = -1, \sigma = +1, k, \lambda)$ in the same BZ only once as the TRIM pair. While for odd pair of surface state crossings (SSC) we have a topologically non-trivial (strong TI), an even number of pairs of SSC corresponds to a topologically trivial (weak TI or conventional insulator) [11]. Thus, there is strong evidence that the system under consideration is a strong topological insulator or a quantum spin Hall (QSH) insulator. We shall show below conclusively, calculating the topological index Z_2 , that the QSH state is possible even when the time reversal symmetry (TRS) is broken due to the finite value of the exchange field M . The material band structures are usually characterized by topological (Kane–Mele) index $Z_2 = +1$ ($\nu = 0$) and $Z_2 = -1$ ($\nu = 1$). The former corresponds to weak TI, while the latter to strong TI. In Figure 2(c) and (d), we have the 3D plots of $\epsilon(s = -1, \sigma = +1, ak, \lambda)$ as a function of the dimensionless wave number (ak) and the intensity of the incident radiation $(\alpha A_0)^2$. As the latter is increased the system makes a crossover to QSH state (blue) starting from quantum anomalous Hall (QAH) region (red). Coming back to Figure 4(a), where the exchange field is $M = 0.3$ and $\alpha A_0 = 0.60$, there is no TRIM pair. Thus, for this value of αA_0 the system is expected to be in quantum anomalous Hall (QAH) phase. A twisted Hilbert space is the important feature of a QSH system or a strong topological insulator. In what follows we show that the Hilbert space of our system is twisted as it is characterized by the Kane–Mele index $Z_2 = -1$ ($\nu = 1$).

The quantized topological numbers, the Kane–Mele index Z_2 (or, the topological invariant ν) [11] for the quantum spin Hall phase and the Chern number C for the quantum anomalous Hall phase, strongly support topological states. We, therefore, feel necessary now to provide a method to calculate the topological invariant ν . This ascertains whether the state attained under intense CPOF is indeed a QSH. For this purpose we require the eigenvectors corresponding to the energy eigenvalues E_j obtainable from Eq. (10). The eigenvectors are Bloch states given by

$$|\psi^{(\alpha)}(k, b)\rangle = \eta_\alpha^{-1/2}(k, b) \begin{pmatrix} \varphi_1^\alpha(k, b) \\ \varphi_2^\alpha(k, b) \\ \varphi_3^\alpha(k, b) \\ \varphi_4^\alpha(k, b) \end{pmatrix}, \quad \alpha = 1, 2, 3, 4, \quad (12)$$

$$\eta_\alpha(k, b) = |\varphi_1^\alpha(k, b)|^2 + |\varphi_2^\alpha(k, b)|^2 + |\varphi_3^\alpha(k, b)|^2 + |\varphi_4^\alpha(k, b)|^2$$

$$\varphi_1^\alpha(k) = 1, \quad \varphi_n^\alpha(k, b) = \Delta_n^{(\alpha)}(k, b) / \Delta^{(\alpha)}(k, b), \quad n = 2, 3, 4$$

$$\Delta^{(\alpha)}(k, b) = (\pm 2iM\eta\widetilde{A}_1cb)(\widetilde{A}_1ak_-), \quad k_- = k_x - ik_y, \quad (13)$$

$$\Delta_2^{(\alpha)}(k, b) = ((\widetilde{A}_1 ak_-))[(\widetilde{A}_1 ak)^2 - (\eta \widetilde{A}_1 cb)^2] - \left((E_j - \epsilon(\overline{k, b}))^2 - (M + \vartheta(\overline{k, b}))^2 \right)$$

$$\Delta_3^{(\alpha)}(k, b) = (\eta \widetilde{A}_1 cb)^2 \{E_j(s, \sigma, k, b) - \epsilon(\overline{k, b}) + M + \vartheta(\overline{k, b})\}$$

$$- \left((E_j(s, \sigma, k, b) - \epsilon(\overline{k, b}))^2 - (M + \vartheta(\overline{k, b}))^2 + (\widetilde{A}_1 ak)^2 \right) \times \{E_j - \epsilon(\overline{k, b}) - M + \vartheta(\overline{k, b})\}$$

$$\Delta_4^{(\alpha)}(k, \lambda) = (\mp i \eta \widetilde{A}_1 cb) ((\widetilde{A}_1 ak)^2 + (\eta \widetilde{A}_1 cb)^2) -$$

$$(\mp i \eta \widetilde{A}_1 cb) \{ (E_j(s, \sigma, k, b) - \epsilon(\overline{k, b}) - M)^2 - \vartheta^2(\overline{k, b}) \} \quad (14)$$

The Hamiltonian $H(k)$ in Eq.(1) satisfies $\Theta^{-1}H(-k)\Theta = H(k)$ for $M=0$, where, for a spin 1/2 particle, the time reversal operator Θ assumes the form $\Theta = I \otimes \sigma_y K$. The symbol I stands for 2×2 identity matrix, σ_j are Pauli matrices on two dimensional \mathbf{k} -space, and the operator K corresponds to the complex conjugation. We consider now a matrix representation of the TR operator In the Bloch wave function basis, the matrix representation of Θ is $\vartheta_{\alpha\beta}(k, b) = \langle \psi^{(\alpha)}(-k, b) | \Theta | \psi^{(\beta)}(k, b) \rangle$, where α and β are band indices. Upon using (11) one can easily show that $\vartheta_{\alpha\beta}(k)$ is a unitary matrix. Quite interestingly, we also find that it has the property:

$$\vartheta_{\alpha\beta}(-k) = i \left[\varphi_2^{*\beta}(k) - \varphi_2^{*\alpha}(-k) + \varphi_4^{*\beta}(k) \varphi_3^{*\alpha}(-k) - \varphi_3^{*\beta}(k) \varphi_4^{*\alpha}(-k) \right] = -\vartheta_{\beta\alpha}(k) \quad (15)$$

which implies that at a \mathbf{k}_{trim} the matrix $\vartheta_{\alpha\beta}(\mathbf{k}_{trim})$ becomes anti-symmetric. As in Floquet theory above, we assume $H[t+T] = H[t]$ by taking the time-dependence for granted. We now consider the green (spin-down) and red bands (spin-up) in Figure 4 and represent their Bloch wave functions by $|\psi^{(2)}(k, t)\rangle$ and $|\psi^{(3)}(k, t)\rangle$, respectively. For this two-band system, the total charge polarizations P may be written as $P = P_2 + P_3$, where

$$P_2 = \int_{-\pi}^{\pi} \frac{dk}{2\pi} c_{22}(k), \quad P_3 = \int_{-\pi}^{\pi} \frac{dk}{2\pi} c_{33}(k). \quad (16)$$

The integrands $c_{jj}(k)$ ($j = 2, 3$) are the Berry connections $\mathbf{A}_j(k) = \{-i \langle \psi^{(j)}(k) | \nabla_k | \psi^{(j)}(k) \rangle\}$. The charge polarization difference between the spin-up and the spin-down quasiparticle bands may be defined as $P_{diff} = P_2 - P_3 = 2P_2 - P$. Furthermore, it may be easily verified that the time-reversed version of the Bloch wave functions by $|\psi^{(3)}(k, t)\rangle$ is equal to $|\psi^{(2)}(-k, t)\rangle$ save for a phase factor. Thus, we can write the time reversed state of $|\psi^{(3)}(k, t)\rangle = e^{-i\gamma(k)} |\psi^{(2)}(-k, t)\rangle$ and, similarly, the time reversed state of $|\psi^{(2)}(k, t)\rangle = -e^{-i\gamma(-k)} |\psi^{(3)}(-k, t)\rangle$ at $t=0$ and $t=T/2$ where $\gamma(k) = i \log \vartheta_{23}(k)$. The Bloch functions $|\psi^{(j)}(k, t)\rangle$ correspond to maps from the 2D phase space (k, t) to the Hilbert space. Furthermore, it is quite straightforward to show that the Berry connections satisfy $c_{22}(-k) = c_{33}(k) - \frac{\partial}{\partial k} \gamma(k)$. In terms of the total polarization density

$$\bar{R}(k) = c_{22}(k) + c_{33}(k) = tr(c(k)) \quad (17)$$

one can write $P_2 = \int_0^\pi \frac{dk}{2\pi} \bar{R}(k) - \frac{i}{2\pi} [\gamma(\pi) - \gamma(0)]$. After a lengthy but straightforward algebra, we find

$$P_{diff} = i \int_0^\pi \frac{dk}{2\pi} \frac{\partial}{\partial k} \log(\det[\vartheta(k)]) - \frac{i}{\pi} \log \frac{\vartheta_{23}(\pi)}{\vartheta_{23}(0)} = \frac{i}{\pi} \cdot \frac{1}{2} \log \frac{\det[\vartheta(\pi)]}{\det[\vartheta(0)]} - \frac{i}{\pi} \log \frac{\vartheta_{23}(\pi)}{\vartheta_{23}(0)}. \quad (18)$$

This leads us to the expression $P_{diff} = \frac{1}{i\pi} \log \left(\frac{\sqrt{\vartheta_{23}(0)^2}}{\vartheta_{23}(0)} \cdot \frac{\vartheta_{23}(\pi)}{\sqrt{\vartheta_{23}(\pi)^2}} \right)$. The argument of the logarithmic term in the right-hand side is +1 or -1. This means P_{diff} is either 0 or 1 (mod 2). The two values of P_{diff} are two different polarization states which the system can assume at $t = 0$ and $t = T/2$. As in ref.[11], the Hilbert space, referred to above, could be separated into two parts depending on the difference in P_{diff} between $t = 0$ and $t = T/2$. This leads to introduction of a quantity $\nu \equiv (P_{tr}(T/2) - P_{tr}(0))$ specified only in mod 2. The triviality of the Hilbert space is represented by $\nu = 0$, while the nontriviality (twisted) corresponds to $\nu = 1$. The system band structures, equivalently, are characterized by $Z_2 = +1$ ($\nu = 0$) and $Z_2 = -1$ ($\nu = 1$). Upon using the expression, $P_{diff} = \frac{1}{i\pi} \log \left(\frac{\sqrt{\vartheta_{23}(0)^2}}{\vartheta_{23}(0)} \cdot \frac{\vartheta_{23}(\pi)}{\sqrt{\vartheta_{23}(\pi)^2}} \right)$, we obtain

$$(-1)^\nu = \prod_j \frac{\vartheta_{23}(ak_{trim}^{(j)})}{\sqrt{\vartheta_{23}(ak_{trim}^{(j)})^2}}. \quad (19)$$

We have found ak_{trim} in Figure 2 (b), A fairly straightforward calculation using the fact that at a k_{trim} the matrix $\vartheta_{\alpha\beta}(k_{trim})$ becomes anti-symmetric convinces us $\vartheta_{23}(ak_{trim}) = -\vartheta_{32}(ak_{trim})$. The square root of the square of the former is $\vartheta_{32}(k_{trim})$. As ν turns out to be 1 or $Z_2 = -1$ (strong TI or QSH phase) when the intensity of incident radiation ~ 0.8 with $M \neq 0$, this is the conclusive evidence of the Hilbert space being twisted in this case. The physical consequence of this nontriviality is the appearance of topologically-protected surface states [11]. The humps in the graphical representations in Figures 2(c) and 2(d) show that the system under consideration makes a crossover to QSH state from QAH state when the intensity of incident radiation ~ 0.8 with $M \neq 0$. Ergo, we have found that the CPOF induced QSH state is accessible even when the time reversal symmetry (TRS) is broken due to the finite value of the exchange field. The question "whether this crossover is a phase transition" could only be settled through thermodynamic consideration-a future task.

4. Concluding remarks

We have considered the Berry connection in the previous section. The Berry curvature $\Omega^{(j)}(k)$ is curl of the Berry connection in momentum space. In 2D, one writes $\Omega_{xy}^{(j)}(k) = i \left\langle \partial_{k_x} \psi^{(j)}(k) \middle| \partial_{k_y} \psi^{(j)}(k) \right\rangle - i \left\langle \partial_{k_y} \psi^{(j)}(k) \middle| \partial_{k_x} \psi^{(j)}(k) \right\rangle$. It is a second-rank, anti-symmetric tensor and becomes zero in the cases where the system is both TRS and inversion symmetry (IS) compliant. On a quick side note, in order to study the possible quantum anomalous Hall (QAH) effect we need to show non-zero Berry curvature (BC). On account of $M \neq 0$, say in Figure 2(a), BC is non-zero. However, the conclusive evidence of QAH phase comes about from the calculation the Chern number C (TKNN invariant), which needs to be an integer. It is expressed as an integral of the Berry curvature over the two-dimensional Brillouin zone(BZ): $C = 2 \iint_{BZ} \sum_n \Omega_{xy}^{(n)}(k) \frac{d^2k}{(2\pi)^2}$. In a future publication we take up the issue of the C calculation for the present system.

We have derived here an effective Hamiltonian for the surface states of a topological insulator thin film incorporating the effect of the normal incidence of POF on the film using the Floquet theory in the high-frequency limit. We found that the surface of the system has states, which come in an odd number of Kramers' doublets when intensity of radiation attains a critical value, as in Figure 4(b). These anti-clockwise/clockwise circling states are carrying spin down/up, or vice versa, depending on the orientation of the magnetic field that enters the spin-orbit interaction (included in section 2). The edge states appear as a consequence of the cyclotron orbits induced by the field, which are naturally truncated at the physical boundary of the sample. The energy levels of the counter-propagating edge states cross at particular points in the Brillouin zone due to TRS. Therefore, the spectrum cannot be now continuously deformed into that of a trivial band insulator. A related phenomenon has been observed, in materials with inversion and mirror symmetries broken, viz. circular photogalvanic effect (CPGE) [25], wherein circularly polarized light incident onto a two-dimensional electron gas system interface, generates a spin polarized photocurrent, is quite interesting. This is an effective approach to exercise a full optical control, such as the generation and the manipulation, of the spin polarized photocurrent, paving the way towards spintronics applications.

References

- [1] Y. Zhang, C.-X. Liu, X.-L. Qi, X. Dai, Z. Fang, and S.-C. Zhang, Topological insulators in Bi_2Se_3 , Bi_2Te_3 and Sb_2Te_3 with a single Dirac cone on the surface, *Nat. Phys.* 5 (2009) 438.
- [2] C. Z. Chang, J. Zhang, X. Feng, J. Shen, Z. Zhang, M. Guo, K. Li, Y. Ou, P. Wei, L. L. Wang, Z. Q. Ji, Y. Feng, S. Ji, X. Chen, J. Jia, X. Dai, Z. Fang, S. C. Zhang, K. He, Y. Wang, L. Lu, X. C. Ma, and Q. K. Xue, Experimental Observation of the Quantum Anomalous Hall Effect in a Magnetic Topological Insulator, *Science* 340 (2013) 167.
- [3] S. Sajad Dabiri, Hosein Cheraghchi, and Ali Sadeghi, Light-induced topological phases in thin films of magnetically doped topological insulators, *Phys. Rev. B* 103(2021) 205130.
- [4] H.-X. Zhu, T.-T. Wang, J.-S. Gao, S. Li, Y.-J. Sun, G.-L. Liu, Floquet Topological Insulator in the BHZ Model with the Polarized Optical Field, *Chin. Phys. Lett.* 31(2014) 030503.
- [5] Chao-Xing Liu, Xiao-Liang Qi, HaiJun Zhang, Xi Dai, Zhong Fang, and Shou-Cheng Zhang, Model Hamiltonian for topological insulators, *Phys. Rev. B* 82, (2010) 045122.
- [6] H.-Z. Lu, A. Zhao, and S.-Q. Shen, Quantum Transport in Magnetic Topological Insulator Thin Films, *Phys. Rev. Lett.* 111, (2013) 146802.
- [7] H. Li, L. Sheng, D. N. Sheng, and D. Y. Xing, Chern number of thin films of the topological insulator Bi_2Se_3 , *Phys. Rev. B* 82, (2010)165104.
- [8] H.-Z. Lu, W.-Y. Shan, W. Yao, Q. Niu, and S.-Q. Shen, Massive Dirac fermions and spin physics in an ultrathin film of topological insulator, *Phys. Rev. B* 81(2010) 115407.
- [9] X.-L. Du, R. Chen, R. Wang, and D.-H. Xu, Weyl nodes with higher-order topology in an optically driven nodal line semimetal, *Phys. Rev. B* 105(2022) L081102.
- [10] Zhen Ning, Baobing Zheng, Dong-Hui Xu, Rui Wang, Photoinduced Quantum Anomalous Hall States in the Topological Anderson Insulator, *Phys. Rev. B* 105(2022) 035103.
- [11] L. Fu and C. L. Kane: *Phys. Rev. B* 74 195312(2006).
- [12] S.Yin, E. Galiffi, and A. Alù, Floquet metamaterials. *eLight* 2, 8 (2022). <https://doi.org/10.1186/s43593-022-00015-1>
- [13] P. M. Blekher, H. R. Jauslin, and J. L. Lebowitz, *Journal of Statistical Physics*, Vol. 68, Nos. 1-2 (1992).
- [14] Hartstein, M.; Toews, W.H.; Hsu, Y.T.; Zeng, B.; Chen, X.; Hatnean, M.C.; Zhang, Q.R.; Nakamura, S.; Padgett, A.S.; Rodway-Gant, G.; et al.,*Nat. Phys.* 14, 166–172(2018).
- [15] L. Li, C. H. Lee, and J. Gong, *Phys. Rev. Lett.* 121, 036401 (2018).
- [16] W. Zhu, M. Umer, and J. Gong, *Phys. Rev. Research* 3, L032026 (2021).

- [17] X. Liu, P. Tang, H. Hübener, U. De Giovannini, W. Duan, and A. Rubio, arXiv preprint arXiv:2106.06977 (2021).
- [18] F. Qin, R. Chen, and H.-Z. Lu, *J. Phys. Condens. Matter* 34, 225001 (2022).
- [19] A. A. Pervishko, D. Yudin, and I. A. Shelykh, Impact of high-frequency pumping on anomalous finite-size effects in three-dimensional topological insulators, *Phys. Rev. B* 97, 075420 (2018).
- [20] R. Chen, B. Zhou, and D.-H. Xu, Floquet Weyl semimetals in light-irradiated type-II and hybrid line node semimetals, *Phys. Rev. B* 97, 155152 (2018).
- [21] R. Chen, D.-H. Xu, and B. Zhou, Floquet topological insulator phase in a Weyl semimetal thin film with disorder, *Phys. Rev. B* 98, 235159 (2018).
- [22] N. Goldman and J. Dalibard, Periodically Driven Quantum Systems: Effective Hamiltonians and Engineered Gauge Fields, *Phys. Rev. X* 4, 031027 (2014).
- [23] A. Eckardt and E. Anisimovas, High-frequency approximation for periodically driven quantum systems from a Floquet-space perspective, *New J. Phys.* 17, 093039 (2015).
- [24] M. Bukov, L. D'Alessio, and A. Polkovnikov, Universal high-frequency behavior of periodically driven systems: from dynamical stabilization to Floquet engineering, *Adv. Phys.* 64, 139 (2015).
- [25] H. Zhang, J. Yao, J. Shao, H. Li, S. Li, D. Bao, C. Wang, G. Yang, *Sci. Rep.* 4, 5876 (2014).
-

ACCEPTED